

Supplementary material

Molecular composition of urban organic aerosols on clear and hazy days in Beijing: a comparative study using FT-ICR MS

Bin Jiang,^A Bin Yu Kuang,^B Yongmei Liang,^{A,C} Jingyi Zhang,^A X. H. Hilda Huang,^B Chunming Xu,^A Jian Zhen Yu^{B,C} and Quan Shi^{A,C}

^AState Key Laboratory of Heavy Oil Processing, China University of Petroleum, Changping District, Beijing 102249, China.

^BDepartment of Chemistry, Hong Kong University of Science and Technology, Clear Water Bay, Kowloon, Hong Kong, China.

^CCorresponding authors. Email: ymliang@cup.edu.cn; chjianyu@ust.hk, sq@cup.edu.cn

Appendix S1. Experimental details of chemical components analysis

Major components analysis

Organic carbon (OC) and elemental carbon (EC) were analyzed using a thermal/optical transmittance (TOT) method on an Aerosol OCEC analyzer (Model: 2001A, Desert Research Institute, USA). The analysis protocol follows the ACE-Asia protocol,^[1] which is a variant of National Institute for Occupational Safety and Health (NIOSH) protocol.^[2] Water-soluble inorganic ions (Na^+ , NH_4^+ , K^+ , Mg^{2+} , Ca^{2+} , Cl^- , NO_3^- , SO_4^{2-} , and oxalate) extracted from portions of the filters using double de-ionized water, were analyzed by an Ion Chromatograph (IC) (Dionex DX-500, Thermo Fisher Scientific, MA, USA).^[3] Water-soluble organic carbon (WSOC) were quantified using a total organic carbon (TOC) analyzer equipped with a nondispersive infrared detector (Shimadzu TOC-VCPH, Japan).^[4]

Anhydrosugars analysis

Three anhydrosugars (levoglucosan, mannosan, and galactosan) are tracers of biomass burning aerosols. They were analyzed using a high-performance anion-exchange chromatography with a pulsed amperometric detection method.^[5] The measurement was carried out on a Dionex DX-500 series ion chromatograph (Sunnyvale, CA, USA).^[4]

Non-polar organic compounds (NPOCs) analysis

Small portions (2-3 cm²) of the filter samples were used for NPOCs (including polycyclic aromatic hydrocarbons (PAHs), hopanes, and alkanes) analysis by a method that couples in-injection port thermal desorption with gas chromatography/ mass spectrometric detection (TD-GC-MS) (Agilent 7890A GC/5975C MS).^[6]

Table S1. Meteorological data of the sampling days

Sample	Average Temperature	Average Humidity	Wind
20141013_clear	12 °C	24%	light air
20141101_clear	11 °C	94%	gentle breeze
20141105_clear	12 °C	80%	gentle breeze
20141211_clear	0 °C	36%	gentle breeze
20141119_hazy	6 °C	67%	light air
20141120_hazy	5 °C	84%	light air
20141126_hazy	16 °C	85%	light air
20141218_hazy	1 °C	64%	light air

Table S2. The results of TD-GC-MS. The unit is ng/m³

Compound	20141013_ clear	20141101_ clear	20141105_ clear	20141211_ clear	20141119_ hazy	20141120_ hazy	20141126_ hazy	20141218_ hazy
PAHs								
phenanthrene	1.04	0.94	1.12	5.46	6.64	8.91	7.33	24.88
anthracene	2.11	2.07	2.07	10.80	19.33	17.39	16.99	52.16
fluoranthene	1.15	0.91	0.95	3.25	4.86	4.72	3.86	10.39
pyrene	1.24	1.04	1.01	3.95	6.12	6.50	5.01	13.31
benzo[c]phenanthrene	0.24	0.25	0.23	0.49	1.08	1.24	1.18	2.45
benz[a]anthracene	0.76	0.74	0.63	2.81	1.07	0.70	0.57	1.75
chrysene	0.29	0.25	0.36	α	0.95	1.35	0.65	α
triphenylene	0.59	0.56	0.43	1.71	3.14	3.77	4.08	9.55
benzo[b]fluoranthene	0.78	0.74	0.65	1.44	1.85	2.03	2.02	5.95
benzo[k]fluoranthene	0.31	0.30	0.29	0.63	0.85	1.26	0.79	1.57
benzo[a]fluoranthene	0.45	0.42	0.30	1.48	1.23	1.56	1.75	1.08
benzo[e]pyrene	0.53	0.50	0.46	0.80	0.72	0.97	0.83	0.98
benzo[a]pyrene	4.36	3.87	2.72	9.88	5.36	7.08	5.07	20.71
perylene	2.58	2.11	1.52	5.38	2.86	4.24	4.99	α
indeno[1,2,3-cd]pyrene	0.31	0.33	0.29	0.24	0.34	0.34	0.20	α
benzo[ghi]perylene	0.44	0.46	0.40	0.29	0.38	0.36	0.40	α
dibenz[a,h]anthracene	0.23	0.23	0.23	0.21	0.31	0.31	0.22	α
dibenz[a,c]anthracene	0.12	0.13	0.13	0.13	0.18	0.17	0.12	α
picene	0.16	0.17	0.16	α	0.27	0.22	0.16	α
benzo[b]chrysene	0.18	0.18	0.18	α	0.26	0.28	0.19	α
coronene	0.12	0.13	0.12	α	α	α	α	α
dibenzo[a,e]pyrene	0.12	0.14	0.13	α	α	α	α	α
cyclopenta[cd]pyrene	0.16	0.15	0.13	0.33	0.76	0.88	0.80	1.43
Total PAHs	18.26	16.63	14.48	49.27	58.54	64.29	57.21	146.20

Table S2. The results of TD-GC-MS. The unit is ng/m³

Compound	20141013_ clear	20141101_ clear	20141105_ clear	20141211_ clear	20141119_ hazy	20141120_ hazy	20141126_ hazy	20141218_ hazy
Hopanes								
22,29,30-trisnorhopane	0.20	0.28	0.28	0.76	3.29	3.32	4.04	6.20
ab-norhopane (C29ab-hopane)	0.65	0.71	0.74	1.35	6.50	5.36	6.56	11.76
ab-hopane (C30ab-hopane)	0.62	0.68	0.73	0.85	6.08	4.85	5.17	7.07
abS-homohopane (C31abS-hopane)	0.14	0.15	0.15	0.16	1.03	0.87	0.84	0.53
abR-homohopane (C31abR-hopane)	0.40	0.46	0.45	0.71	5.64	4.13	4.64	7.25
aa 20R-cholestane	0.27	0.25	0.28	0.29	1.19	1.06	1.17	1.61
aaa 20R 24R-ethylcholestane	0.23	0.27	0.26	0.65	2.99	3.46	4.17	5.61
abb 20R-cholestane	0.03	0.03	0.03	0.02	0.13	0.08	0.12	0.18
abb 20R 24S-methylcholestane	0.26	0.25	0.26	0.31	2.24	1.86	1.90	3.16
abb 20R 24R-ethylcholestane	0.08	0.10	0.10	0.18	0.88	0.92	1.04	1.00
Total hopanes	2.89	3.18	3.27	5.29	29.97	25.91	29.65	44.38
Alkanes								
n-C17	1.16	2.11	0.65	0.86	4.18	5.02	4.25	7.10
pristane	α	α	α	α	α	α	α	α
n-C18	0.71	0.54	0.08	1.74	2.21	2.57	2.54	6.44
phytane	0.79	0.61	0.19	0.94	1.52	2.61	1.75	3.09
n-C19	1.46	0.99	0.77	4.77	4.17	4.49	4.40	14.75

Table S2. The results of TD-GC-MS. The unit is ng/m³

Compound	20141013_ clear	20141101_ clear	20141105_ clear	20141211_ clear	20141119_ hazy	20141120_ hazy	20141126_ hazy	20141218_ hazy
n-C20	2.09	1.23	0.75	7.34	10.46	7.82	7.65	37.20
n-C21	4.09	2.77	2.13	8.40	15.08	17.08	20.36	58.36
n-C22	5.16	3.89	3.94	9.93	26.79	32.58	36.25	71.42
n-C23	5.64	4.64	5.47	10.38	34.68	39.38	40.39	68.68
n-C24	4.70	4.19	4.87	9.13	30.89	37.11	38.35	64.88
n-C25	5.71	5.81	7.05	9.95	30.25	35.94	37.35	67.15
n-C26	4.14	3.47	4.51	5.95	21.68	24.57	25.07	39.39
squalane	0.01	0.04	0.22	α	0.80	0.61	1.04	0.41
n-C27	7.11	7.54	8.69	6.39	21.82	25.17	22.73	34.67
n-C28	2.74	2.53	3.51	2.79	12.96	14.70	13.01	19.19
n-C29	7.85	8.28	10.80	6.38	23.85	24.84	19.33	24.77
n-C30	1.72	1.39	2.21	1.55	10.33	10.12	8.70	11.25
n-C31	5.58	5.01	7.32	6.05	6.64	15.07	11.19	16.24
n-C32	1.34	1.12	1.60	1.08	5.93	7.41	6.31	2.91
n-C33	2.10	1.71	2.60	1.86	α	10.48	7.56	2.94
n-C34	0.77	0.78	1.04	0.76	α	4.24	2.92	α
n-C35	0.86	0.87	1.11	0.86	α	4.30	2.14	α
n-C36	0.79	0.84	0.95	0.81	α	2.94	1.75	α
n-C37	0.89	0.91	0.97	0.88	α	2.68	α	α
n-C38	0.95	0.99	1.05	0.94	α	2.48	α	α
n-C39	α	1.10	1.14	α	α	2.31	α	α

^aBelow the detection limit.

Table S3. Identification of Singly Charged Ions at Nominal m/z 319

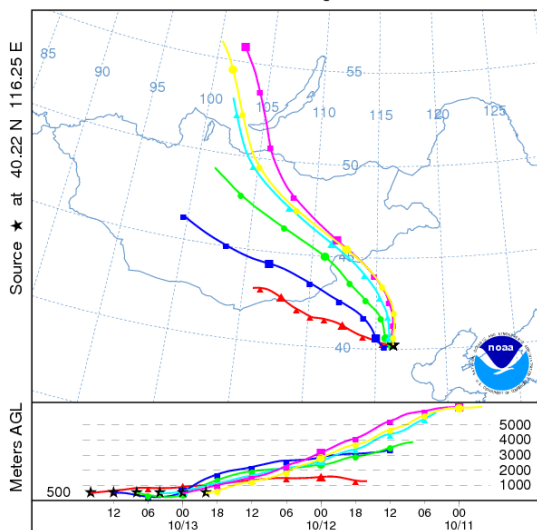
formula [M-H]-	observed mass (Da)	theoretical mass (Da)	error (ppm)	S/N	resolving power
C ₂₀ H ₂₁ O ₃	319.22797	319.22787	-0.3	23.5	465625
C ₁₆ H ₃₁ O ₄ S ₁	319.19492	319.19485	-0.2	77.1	471060
C ₁₉ H ₂₇ O ₄	319.19155	319.19148	-0.2	44.5	486919
C ₁₈ H ₂₇ O ₇	319.17633	319.17623	-0.3	28.4	492744
C ₁₅ H ₂₇ O ₅ S ₁	319.15854	319.15847	-0.2	151. 5	477500
C ₁₈ H ₂₃ O ₅	319.15518	319.15510	-0.3	56.0	470080
C ₁₄ H ₂₃ O ₈	319.13992	319.13984	-0.2	16.7	470386
C ₂₁ H ₁₉ O ₃	319.13405	319.13397	-0.2	15.8	547472
C ₁₄ H ₂₃ O ₆ S ₁	319.12214	319.12208	-0.2	129. 0	471058
C ₁₃ H ₁₉ O ₉	319.10352	319.10346	-0.2	30.4	504280
C ₁₇ H ₁₉ O ₆	319.11878	319.11871	-0.2	98.5	491477
C ₂₀ H ₁₅ O ₄	319.09766	319.09758	-0.3	62.1	490254
C ₁₃ H ₁₉ O ₇ S ₁	319.08577	319.08570	-0.2	73.6	478680
C ₁₆ H ₁₅ O ₇	319.08240	319.08233	-0.2	97.9	475215
C ₁₆ H ₁₅ O ₅ S ₁	319.06466	319.06457	-0.3	29.0	457347
C ₁₉ H ₁₁ O ₅	319.06127	319.06120	-0.2	84.8	485696
C ₁₂ H ₁₅ O ₈ S ₁	319.04938	319.04931	-0.2	38.7	505134
C ₁₅ H ₁₁ O ₈	319.04600	319.04594	-0.2	23.6	487621
C ₁₅ H ₁₁ O ₆ S ₁	319.02827	319.02818	-0.3	18.8	516063

Table S4. Identification of Singly Charged Ions at Nominal m/z 312

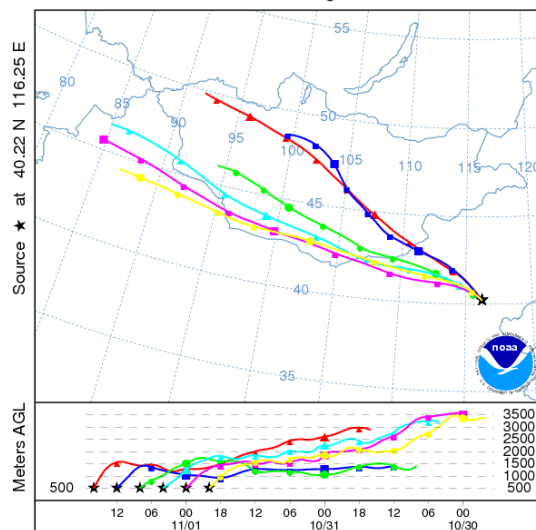
formula [M-H] ⁻	observed mass (Da)	theoretical mass (Da)	error (ppm)	S/N	resolving power
¹³ C ₁ C ₁₇ H ₃₁ O ₄	312.22624	312.22620	-0.1	53.9	534977
C ₁₆ H ₂₆ O ₅ N ₁	312.18174	312.18165	-0.3	9.7	650222
¹³ C ₁ C ₁₆ H ₂₇ O ₃ S ₁	312.17211	311.17188	-0.7	78.1	533027
C ₁₅ H ₂₂ O ₆ N ₁	312.14535	312.14526	-0.3	31.2	529039
C ₁₈ H ₁₈ O ₄ N ₁	312.12426	312.12413	-0.4	30.2	536389
C ₁₁ H ₂₂ O ₇ N ₁ S ₁	312.11237	312.11225	-0.4	260.1	509060
C ₁₄ H ₁₈ O ₇ N ₁	312.10901	312.10888	-0.4	40.6	489869
C ₁₇ H ₁₄ O ₅ N ₁	312.08788	312.08775	-0.4	59.3	500567
C ₁₀ H ₁₈ O ₈ N ₁ S ₁	312.07599	312.07586	-0.4	362.1	507979
C ₁₃ H ₁₄ O ₈ N ₁	312.07264	312.07249	-0.5	52.3	516577
C ₁₆ H ₁₀ O ₆ N ₁	312.05153	312.05136	-0.5	47.5	509324
C ₉ H ₁₄ O ₉ N ₁ S ₁	312.03963	312.03948	-0.5	127.8	508917

Clear days

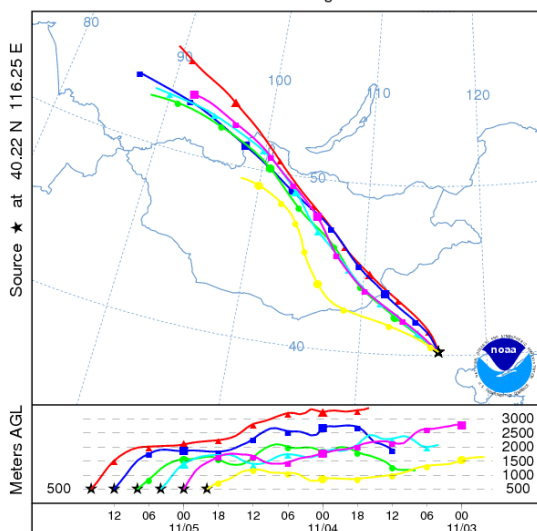
NOAA HYSPLIT MODEL
Backward trajectories ending at 1600 UTC 13 Oct 14
GDAS Meteorological Data



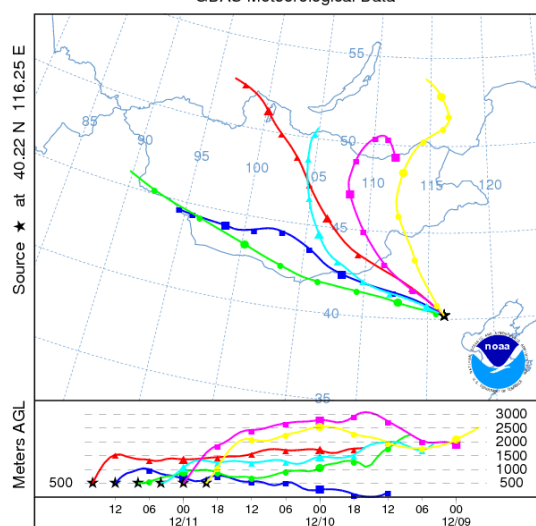
NOAA HYSPLIT MODEL
Backward trajectories ending at 1600 UTC 01 Nov 14
GDAS Meteorological Data



NOAA HYSPLIT MODEL
Backward trajectories ending at 1600 UTC 05 Nov 14
GDAS Meteorological Data



NOAA HYSPLIT MODEL
Backward trajectories ending at 1600 UTC 11 Dec 14
GDAS Meteorological Data



Hazy days

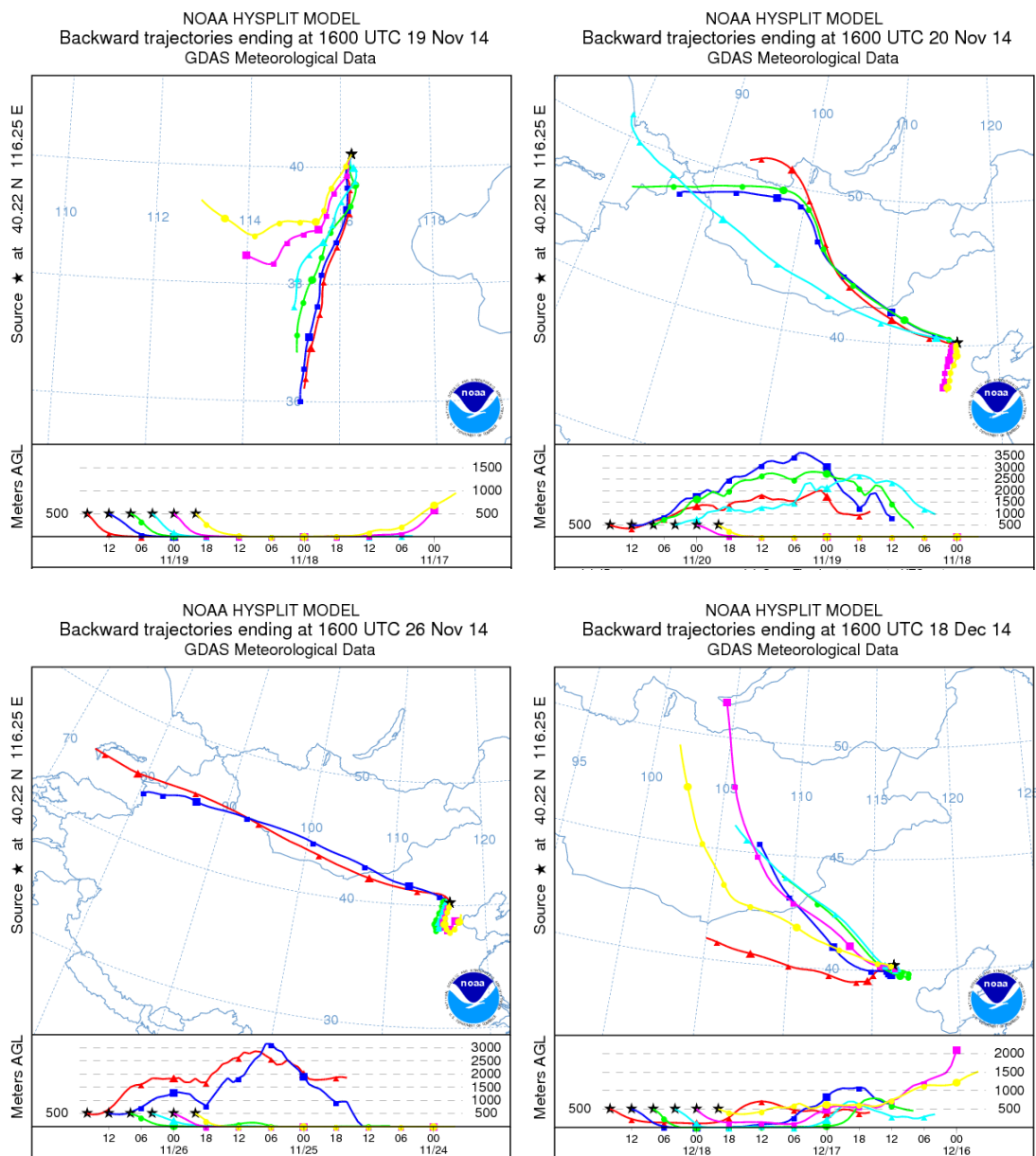


Fig. S1. The 48-hour back trajectories of the 8 sampling days.^[7] The start time of each trajectory in a day is of 4-hour difference. On the clear days, the back trajectories are all directly from the north, which are less polluted areas. On the contrary, on the hazy days, some or all of the back trajectories of that day are from the south, which are industrial polluted areas.

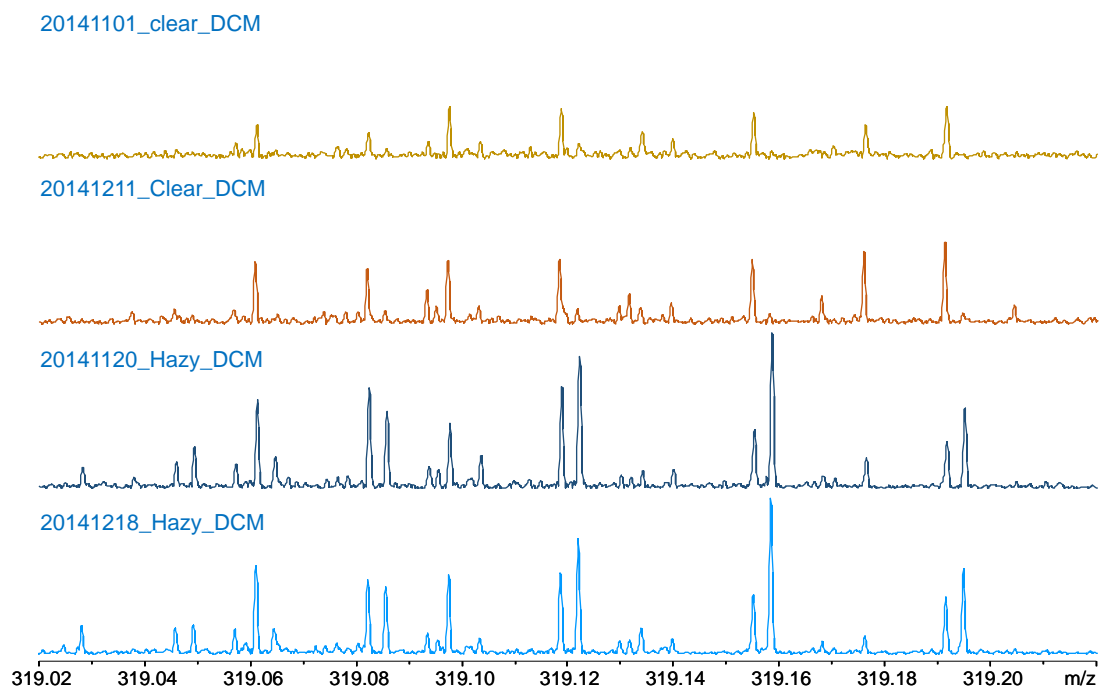


Fig. S2. The mass scale-expanded segments (m/z 319) of $-ESI$ FT-ICR mass spectra for the DCM extracts of aerosols on Nov 1, 20 and Dec 11, 18.

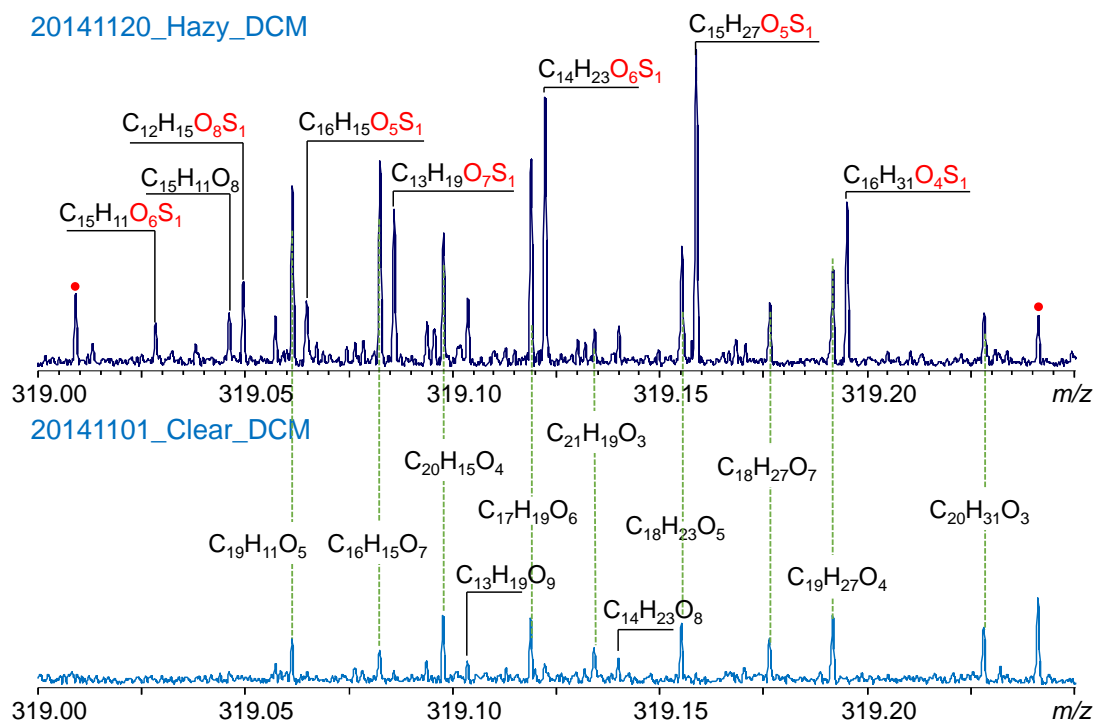


Fig. S3. Mass scale-expanded segments (m/z 319) of $-ESI$ FT-ICR mass spectra for the DCM extracts of aerosols on hazy and clear days. The red dots denote unidentified peaks.

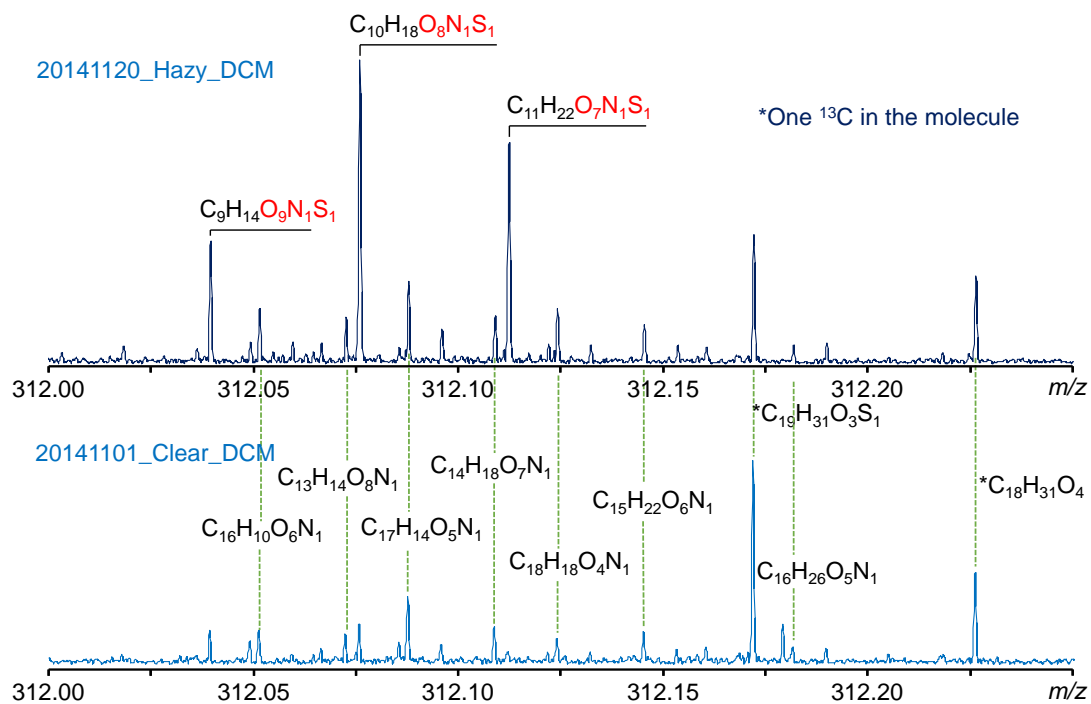


Fig. S4. Mass scale-expanded segments (m/z 312) of $-ESI$ FT-ICR mass spectra for the DCM extracts of aerosols on hazy and clear days.

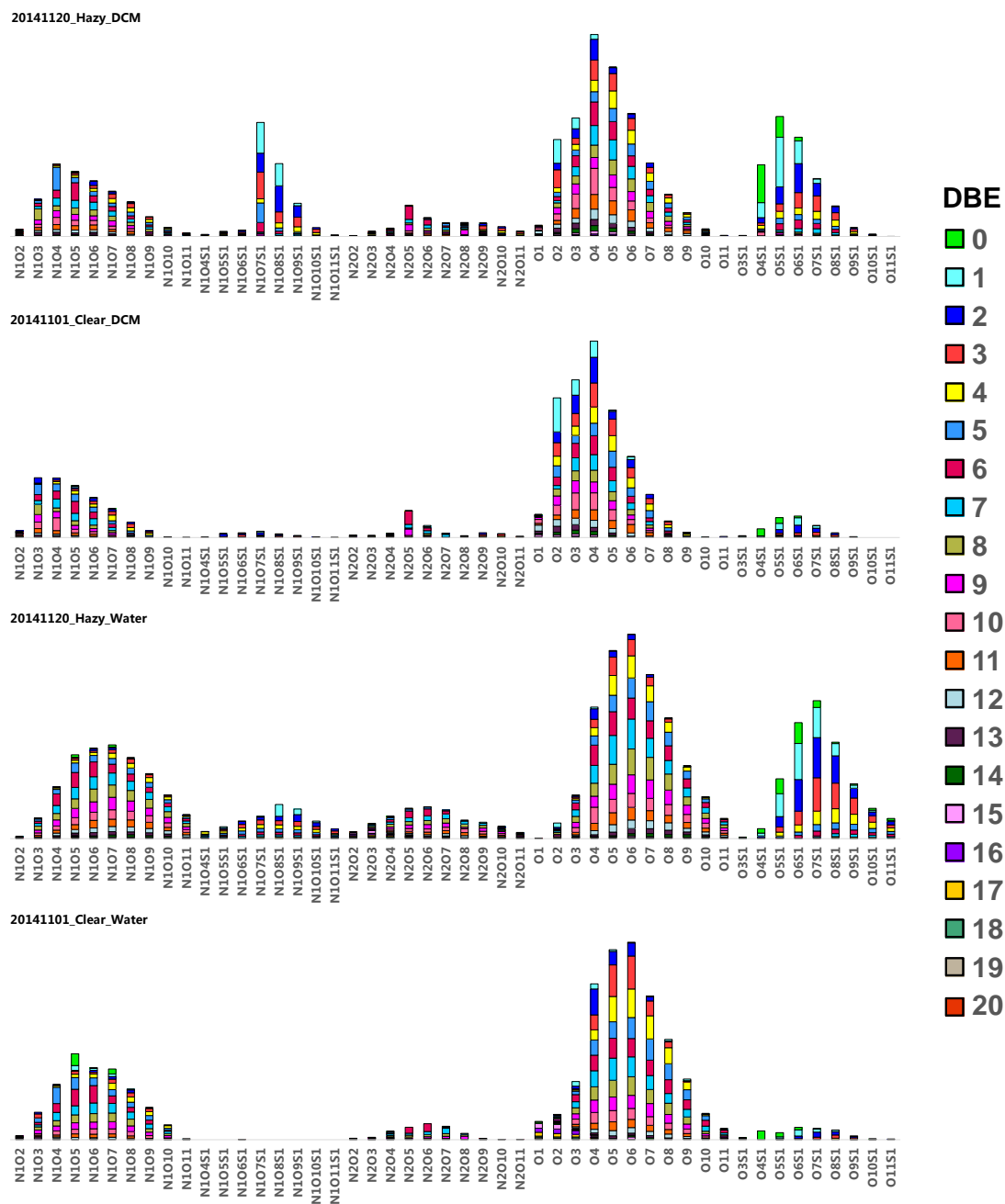


Fig. S5. Relative abundance of O_xN_1 , $O_xN_1S_1$, O_x , O_xS_1 class species for the DCM and water extracts of aerosols on hazy and clear days.

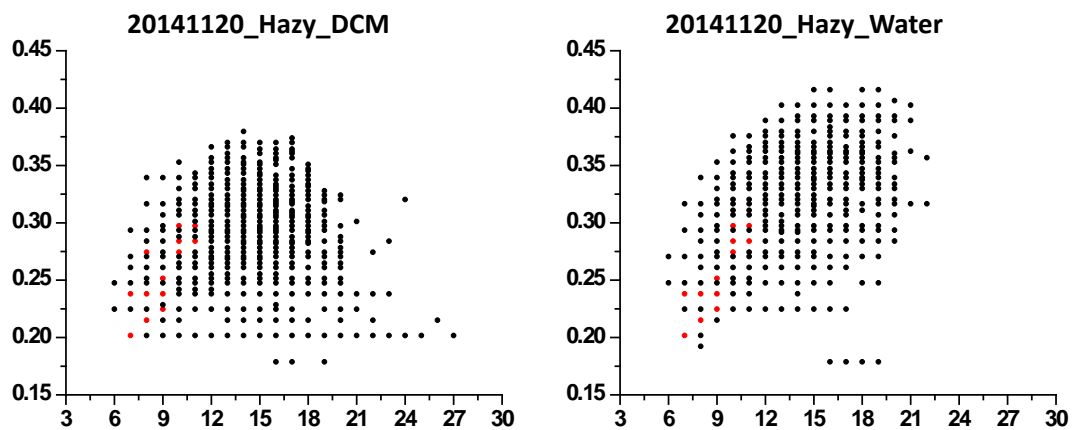


Fig. S6. CH₂ based Kendrick mass defect (KMD) vs carbon numbers for subgroup A in the DCM and water extract of the hazy-day sample. The red dots denote aromatic OS and sulfonates identified in chamber studies by Riva et al.^[8]

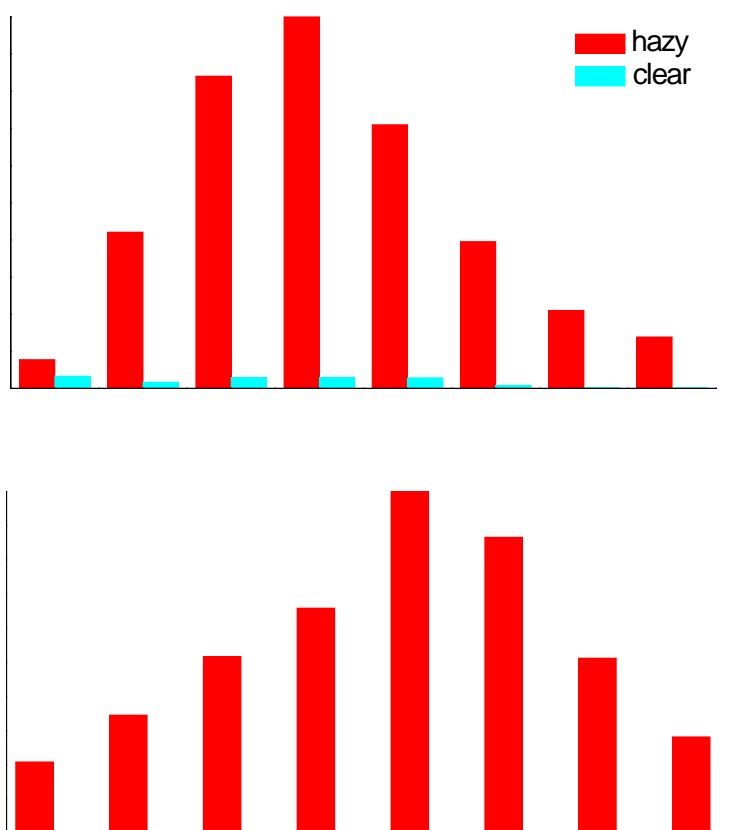


Fig. S7. Relative abundance of O₄S₁-O₁₁S₁ and O₄N₁S₁-O₁₁N₁S₁ class species of the water extracts on hazy and clear day (Normalized by the organosulfate standard).

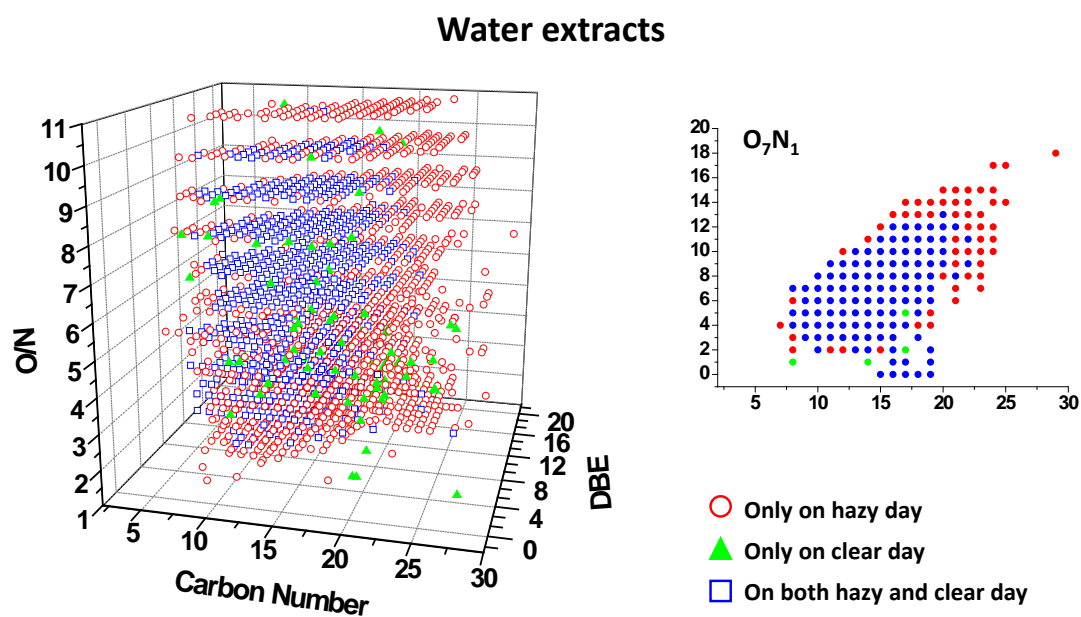


Fig. S8. The 3D plot of DBE, C number and O/N ratio distributions of CHON compounds (including CHON₁ and CHON₂) in the water extracts of the hazy-day and clear-day samples. The insert is iso-abundance plots of DBE versus carbon numbers for O₇N₁ class species. Color-coding indicates the compounds observed only on clear day (green), only on hazy day (red), and on both clear & hazy day (blue).

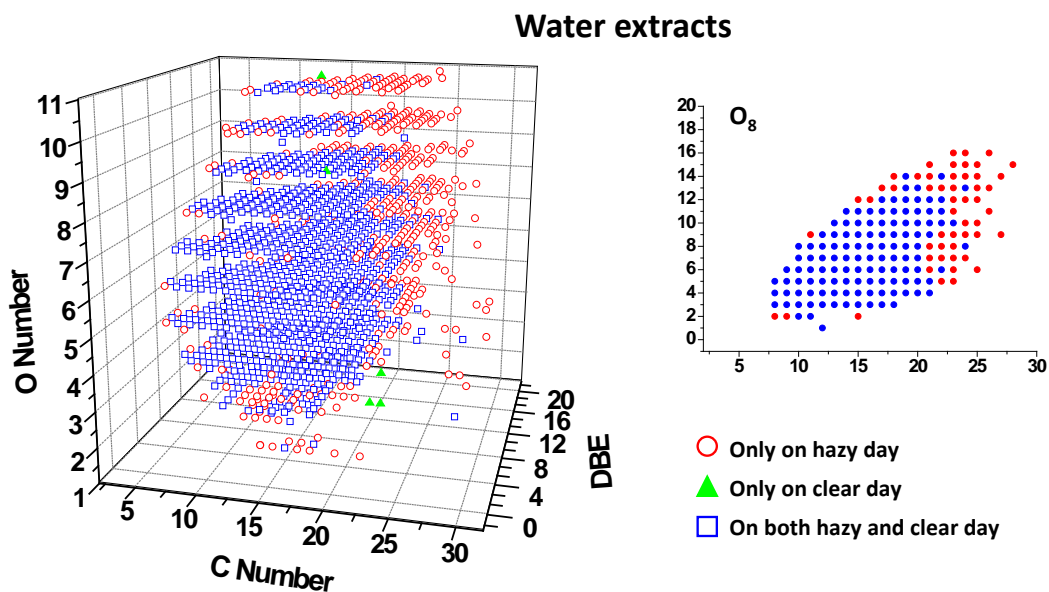


Fig. S9. The 3D plot of DBE, C and O number distributions of the CHO compounds in the water extracts of the hazy-day and clear-day samples. The insert is iso-abundance plots of DBE versus carbon numbers for O₈ class species. Color-coding indicates the compounds observed only on clear day (green), only on hazy day (red), and on both clear & hazy day (blue).

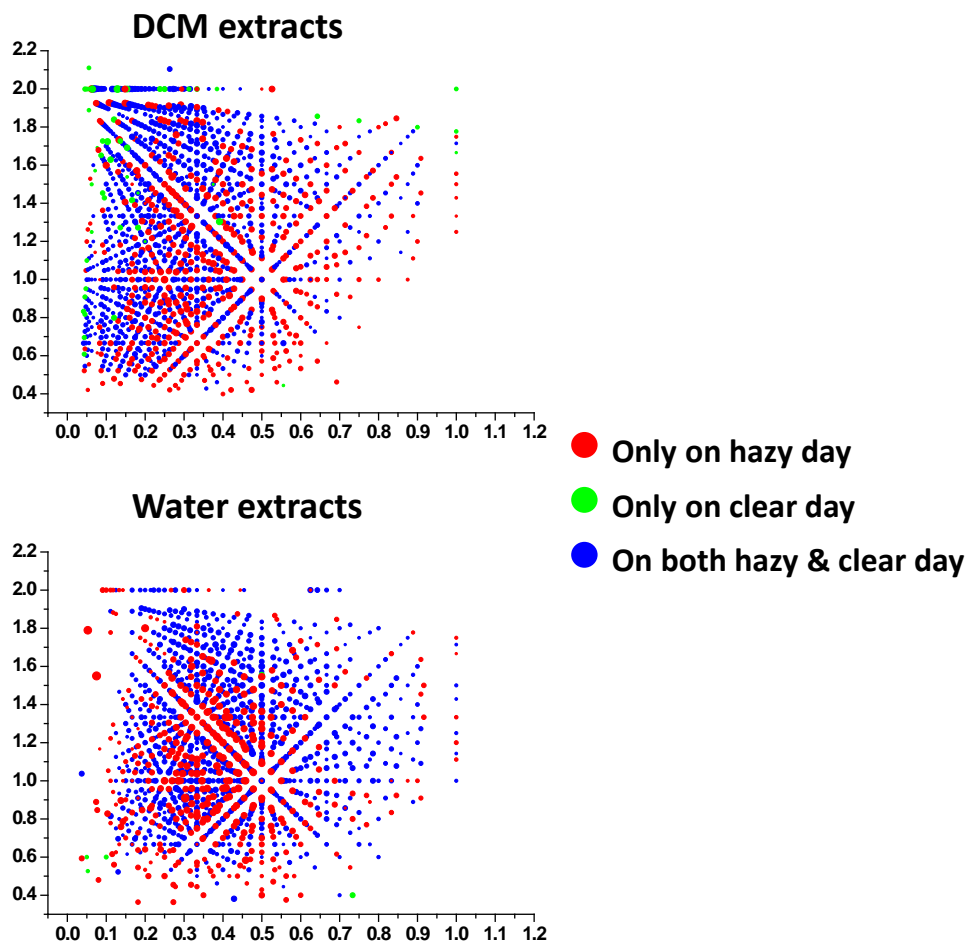


Fig. S10. Van Krevelen diagrams of the CHO compounds in the DCM and water extracts of aerosols on hazy and clear days. Color-coding indicates the compounds observed only on clear day (green), only on hazy day (red), and on both clear & hazy day (blue).

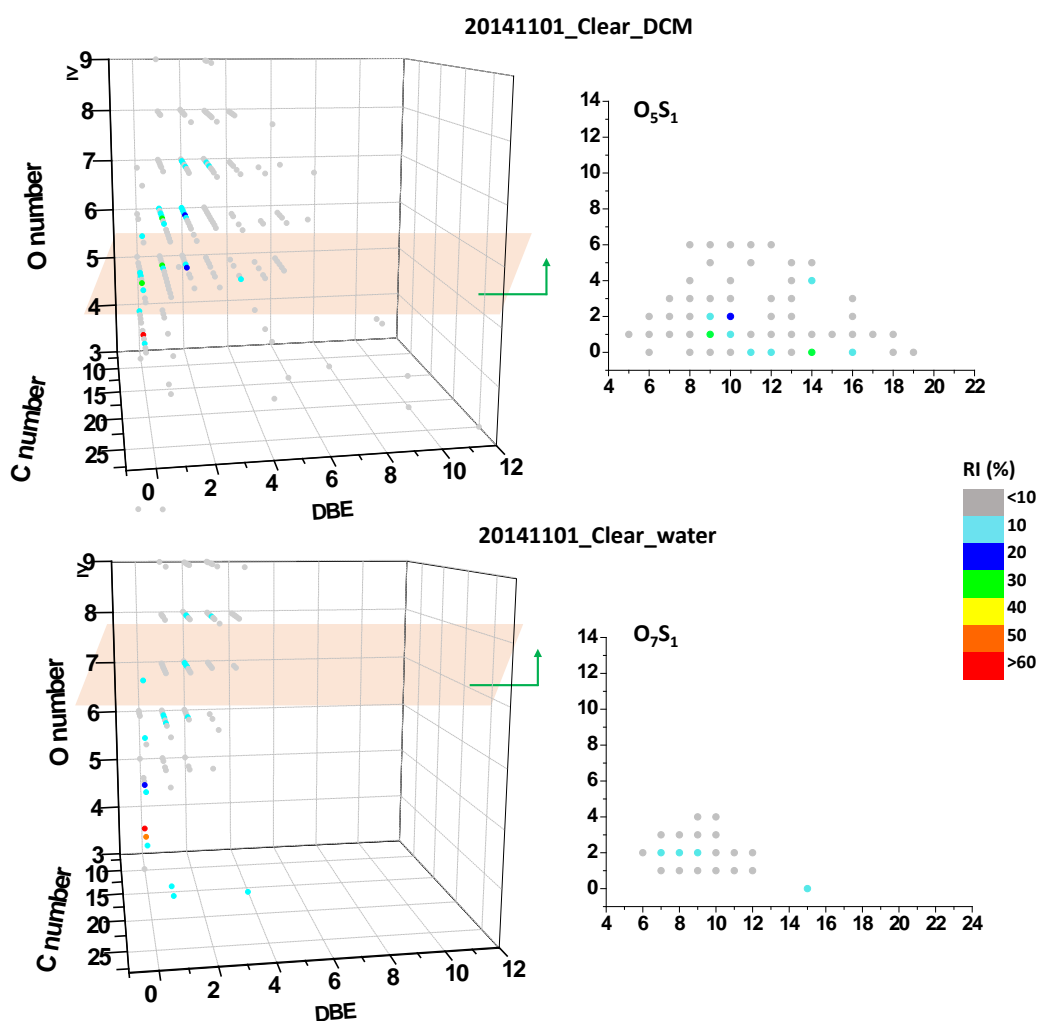


Fig. S11. DBE, C and O number distributions for CHOS compounds in the DCM and water extract of clear-day PM_{2.5}. The inserts are plots of DBE versus carbon numbers for O₅S₁ class species in the DCM extract and O₇S₁ class species in the water extract. The color bar in the figures denotes the relative peak intensities (0-100%). The figure was plotted by OriginPro 8.5.

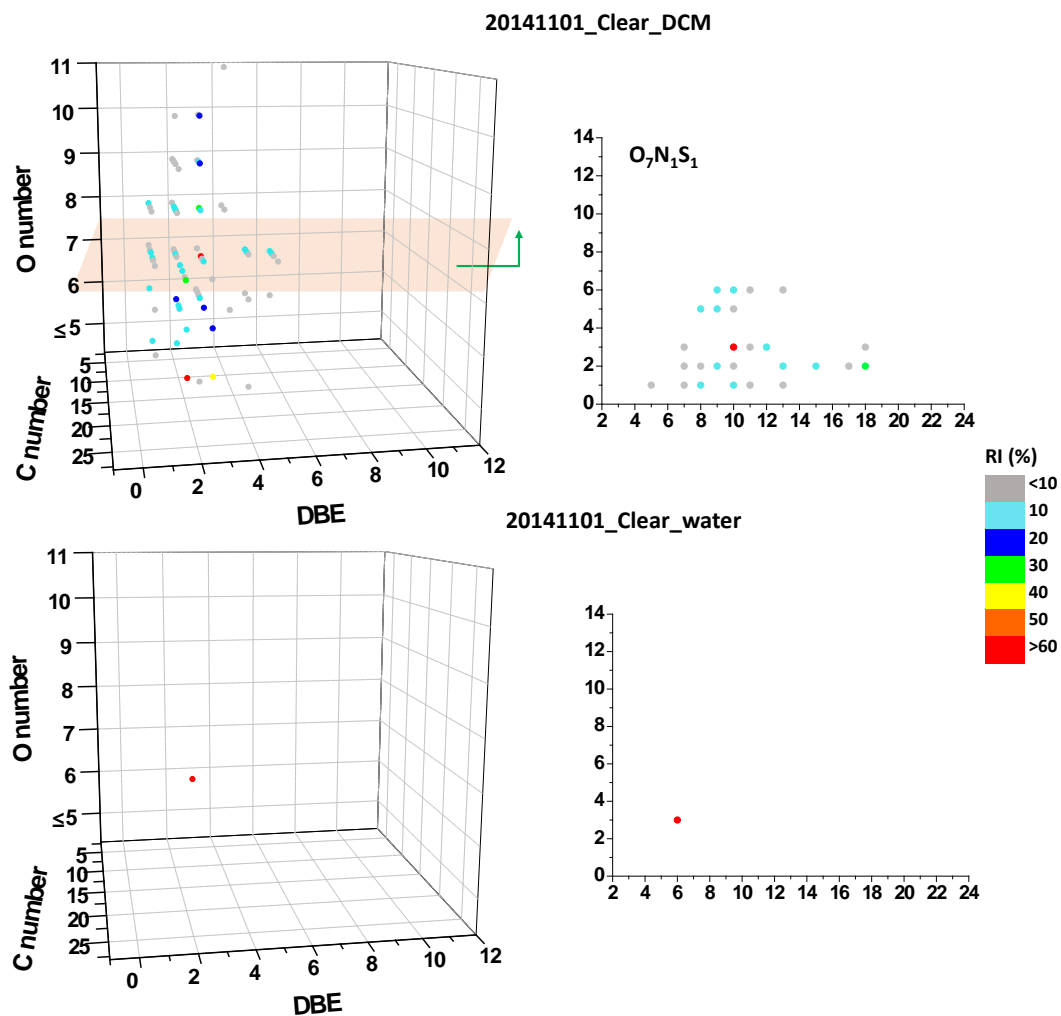


Fig. S12. DBE, C and O number distributions of CHN_1OS compounds in the DCM and water extract of the clear-day $\text{PM}_{2.5}$. The inserts are plots of DBE versus carbon numbers for $\text{O}_7\text{N}_1\text{S}_1$ class species in the DCM extract and $\text{O}_6\text{N}_1\text{S}_1$ class specie in the water extract. The color bar in the figures denote the relative peak intensities (0-100%).

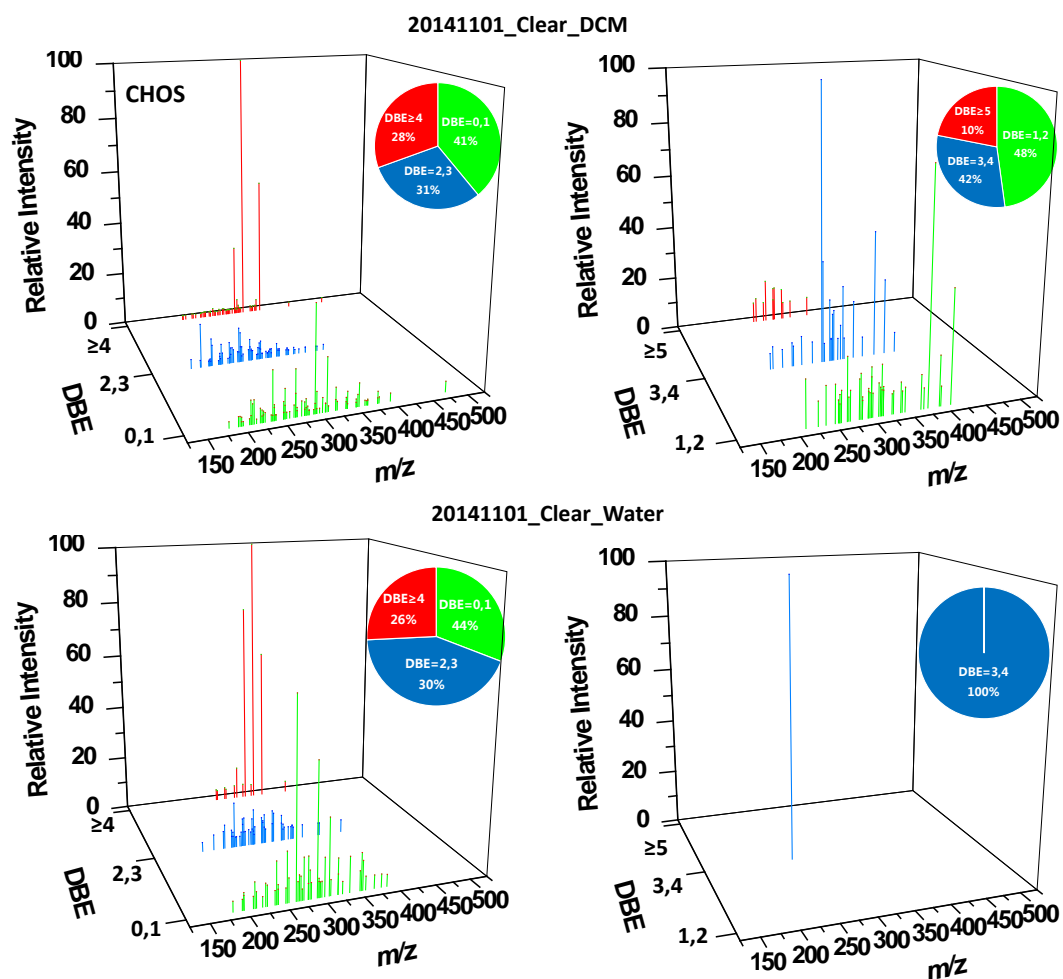


Fig. S13. Reconstructed mass spectrums of CHOS compounds and CHON₁S compounds of different DBEs in the DCM and water extract of the clear-day PM_{2.5}. The ions of CHOS compounds with DBE=0, 1, DBE=2, 3, and DBE≥4 and CHON₁S compounds with DBE=1, 2, DBE=3, 4, and DBE≥5 were denoted by green, blue and red color for enhanced visualization, respectively. The inserted pie charts show the percentage of different DBE groups by intensity, respectively.

References

- [1] J. J. Schauer, B. T. Mader, J. T. Deminter, G. Heidemann, M. S. Bae, J. H. Seinfeld, R. C. Flagan, R. A. Cary, D. Smith, B. J. Huebert, T. Bertram, S. Howell, J. T. Kline, P. Quinn, T. Bates, B. Turpin, H. J. Lim, J. Z. Yu, H. Yang, M. D. Keywood, ACE-Asia intercomparison of a thermal-optical method for the determination of particle-phase organic and elemental carbon. *Environ. Sci. Technol.* **2003**, *37*, 993.
- [2] C. Wu, W. M. Ng, J. X. Huang, D. Wu, J. Z. Yu, Determination of Elemental and Organic Carbon in PM_{2.5} in the Pearl River Delta Region: Inter-Instrument (Sunset vs. DRI Model 2001 Thermal/Optical Carbon Analyzer) and Inter-Protocol Comparisons (IMPROVE vs. ACE-Asia Protocol). *Aerosol. Sci. Tech.* **2012**, *46*, 610.
- [3] X. H. H. Huang, Q. J. Bian, W. M. Ng, P. K. K. Louie, J. Z. Yu, Characterization of PM_{2.5} Major Components and Source Investigation in Suburban Hong Kong: A One Year Monitoring Study. *Aerosol and Air Quality Research.* **2014**, *14*, 237.
- [4] B. Y. Kuang, P. Lin, X. H. H. Huang, J. Z. Yu, Sources of humic-like substances in the Pearl River Delta, China: positive matrix factorization analysis of PM_{2.5} major components and source markers. *Atmos. Chem. Phys.* **2015**, *15*, 1995.
- [5] G. Engling, C. M. Carrico, S. M. Kreidenweis, J. L. Collett, D. E. Day, W. C. Malm, E. Lincoln, W. M. Hao, Y. Iinuma, H. Herrmann, Determination of levoglucosan in biomass combustion aerosol by high-performance anion-exchange chromatography with pulsed amperometric detection. *Atmos. Environ.* **2006**, *40*, S299.
- [6] S. S. H. Ho, J. Z. Yu, J. C. Chow, B. Zielinska, J. G. Watson, E. H. L. Sit, J. J. Schauer, Evaluation of an in-injection port thermal desorption-gas chromatography/mass spectrometry method for analysis of non-polar organic compounds in ambient aerosol samples. *J. Chromatogr. A.* **2008**, *1200*, 217.
- [7] R. R. Draxler, G. D. Rolph, HYSPLIT (HYbrid Single-Particle Lagrangian Integrated Trajectory) Model access via NOAA ARL READY Website (<http://www.arl.noaa.gov/HYSPLIT.php>). NOAA Air Resources Laboratory, College Park, MD. **2011**.
- [8] Matthieu Riva, Sophie Tomaz, Tianqu Cui, Ying-Hsuan Lin, Emilie Perraudin, Avram Gold, Elizabeth A Stone, Eric Villenave, Jason Douglas Surratt, Evidence for an Unrecognized Secondary Anthropogenic Source of Organosulfates and Sulfonates: Gas-Phase Oxidation of Polycyclic Aromatic Hydrocarbons in the Presence of Sulfate Aerosol. *Environ. Sci. Technol.* **2015**, *49*.